

Accumulation of Intracellular Glycogen and Trehalose by *Propionibacterium freudenreichii* under Conditions Mimicking Cheese Ripening in the Cold

Marion Dalmasso,^{a,b} Julie Aubert,^{c,d} Sergine Even,^{a,b} Hélène Falentin,^{a,b} Marie-Bernadette Maillard,^{a,b} Sandrine Parayre,^{a,b} Valentin Loux,^e Jarna Tanskanen,^f and Anne Thierry^{a,b}

INRA, UMR1253 Science et Technologie du Lait et de l'Œuf, Rennes, France^a; Agrocampus Ouest, UMR1253 Science et Technologie du Lait et de l'Œuf, Rennes, France^b; INRA, UMR518 Mathématiques et Informatique Appliquées, Paris, France^c; AgroParisTech, UMR518 Mathématiques et Informatique Appliquées, Paris, France^d; INRA, UR1077 Mathématique, Informatique et Génome, Jouy-en-Josas, France^e; and Valio Ltd., Helsinki, Finland^f

Seven *Propionibacterium freudenreichii* strains exhibited similar responses when placed at 4°C. They slowed down cell machinery, displayed cold stress responses, and rerouted their carbon metabolism toward trehalose and glycogen synthesis, both accumulated in cells. These results highlight the molecular basis of long-term survival of *P. freudenreichii* in the cold.

Propionibacterium freudenreichii is a bacterium of food and probiotic interest, widely used as a ripening culture in the manufacture of Swiss cheese varieties (4, 16). It grows in cheese during ripening at warm temperatures (20 to 24°C) but remains metabolically active during the storage of cheese at low temperatures (10). We previously investigated the adaptation strategies of *P. freudenreichii* type strain CIRM-BIA1^T by -omic approaches under conditions mimicking cheese ripening in the cold (6). Our previous results suggest in particular that CIRM-BIA1^T reroutes its metabolism toward glycogen synthesis. In the present study, we confirmed the actual accumulation of glycogen in cells and investigated the response in the cold of six other *P. freudenreichii* strains.

Choice of strains and culture conditions. The transcriptomic response of six *P. freudenreichii* subsp. *shermanii* strains (CIRM-BIA9, CIRM-BIA118, CIRM-BIA122, and CIRM-BIA123 from CIRM-BIA [Centre International de Ressources Microbiennes—Bactéries d’Intérêt Alimentaire, INRA, Rennes, France] and CIRM-BIA472 and CIRM-BIA482 from Valio Ltd., Helsinki, Finland) was studied during their transfer from 30°C to 4°C under conditions mimicking cheese ripening, previously applied to strain CIRM-BIA1^T (6). All experiments were made in triplicate independent cultures. The six strains were chosen with different sequence types (7) and phenotypes. For example, they produce methylbutanoate and ethyl propionate, two cheese aroma compounds, at concentrations varying by factors of 6 and 12, respectively, depending on the strain (data not shown).

Growth and metabolite production in the cold. All the strains stopped their growth when placed at 4°C, whereas in the control cultures maintained at 30°C, cells went on growing for about 20 h (Fig. 1A). They went on producing propionate and acetate, the two main products of lactate fermentation, but at a markedly lower production rate in the cold (Fig. 1C and D) (3.4 ± 0.6 [mean \pm standard deviation] mM per day at 4°C versus 76 ± 15 mM per day at 30°C, i.e., a $23\text{-} \pm 6$ -fold decrease for propionate). The rate of methylbutanoate production also decreased but at a markedly lower extent (from 69 ± 55 μ M per day at 30°C to 12 ± 12 μ M per day at 4°C, i.e., a mean fold decrease of 7 ± 4) (Fig. 1B).

Transcriptomic approach applied to all strains. Gene expression after an 80-h period at 4°C ($t = 120$ h) was compared to that at 20 h during growth at 30°C for the 6 strains, using the methodology and microarrays previously described for strain CIRM-

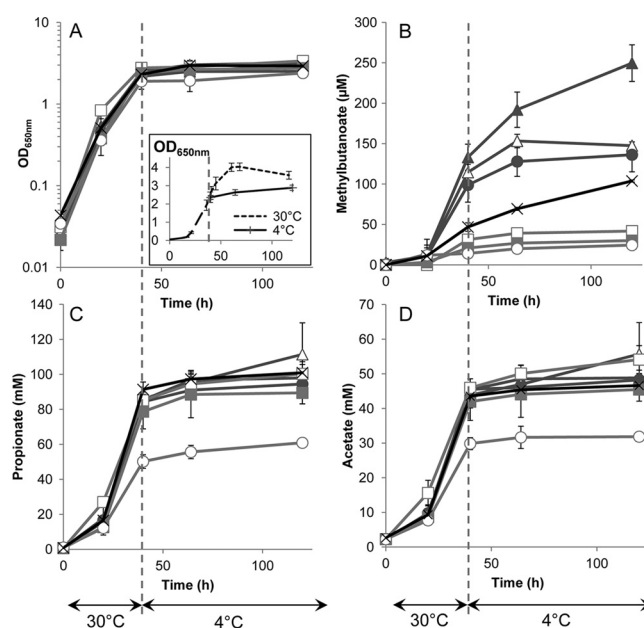


FIG 1 Time course of metabolic activity of seven *P. freudenreichii* strains over a 40-h incubation at 30°C followed by a further 80 h at 4°C. Growth (OD_{650nm}, optical density at 650 nm) (A), concentrations of methylbutanoate (sum of 2-methylbutanoate and 3-methylbutanoate) (B), propionate (C), and acetate (D). Error bars show the standard deviations of the results of triplicate independent experiments. The inset in panel A shows the growth curves at 4°C and 30°C. Values are means for the 7 strains: CIRM-BIA1^T (×), CIRM-BIA9 (△), CIRM-BIA118 (□), CIRM-BIA122 (▲), CIRM-BIA123 (○), CIRM-BIA472 (●), CIRM-BIA482 (■).

BIA1^T (6) (NCBI GEO, <http://www.ncbi.nlm.nih.gov/geo/>, platform accession number GPL13959). The transcriptomic data for

Received 1 March 2012 Accepted 14 June 2012

Published ahead of print 22 June 2012

Address correspondence to Anne Thierry, anne.thierry@rennes.inra.fr.

Copyright © 2012, American Society for Microbiology. All Rights Reserved.

doi:10.1128/AEM.00561-12

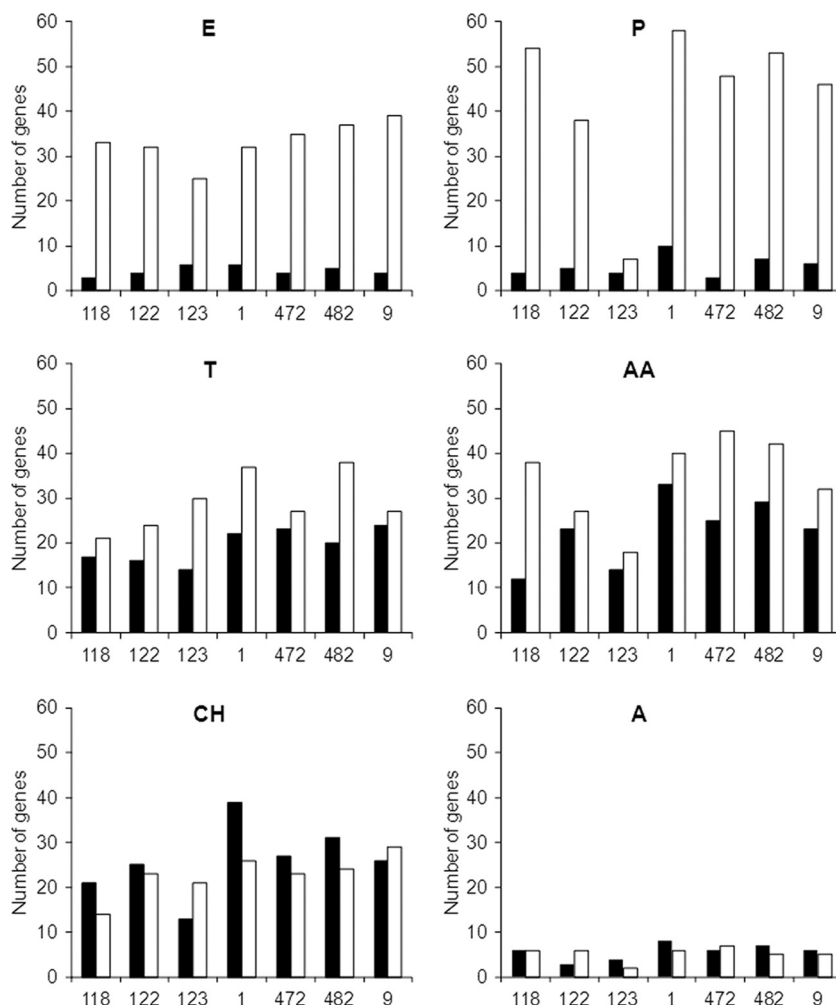


FIG 2 Number of differentially expressed genes (fold change > 1) after 80 h at 4°C in comparison with gene expression at the reference time of 20 h for seven *P. freudenreichii* strains (CIRM-BIA118, -122, -123, -1, -472, -482, and -9). Downregulated (white bars) or upregulated (black bars) genes with known functions are presented according to their metabolic category: E, energy metabolism; P, protein synthesis; T, transport of peptides and inorganic ions; AA, transport and metabolism of amino acids; CH, transport and metabolism of carbohydrates; A, adaptation to atypical conditions.

CIRM-BIA1^T at sampling times 20 h and 3 days (accession number [GSE30841](#)) were added to the new data set (six strains, accession number [GSE34227](#)) to facilitate the comparison between the present and previous results. Microarray data were normalized and analyzed as previously described (6). An analysis of variance (ANOVA) was performed to evaluate the effects of time, strain, and their interactions on expression. Raw *P* values were adjusted for multiple comparisons by the Benjamini-Hochberg procedure. Since the microarray used was designed from the genome of strain CIRM-BIA1^T, we first checked the quality of hybridization with DNA of all the strains used, to avoid any bias in the interpretation of results due to possible mismatches between the oligonucleotides and the DNA sequence of the 6 other strains. DNA was extracted from pure cultures as previously described (10). A signal intensity of >8 (expressed as \log_2) was obtained for all oligonucleotides using DNA from CIRM-BIA1^T, whereas a low signal intensity (<6) was observed using DNA from the other strains for a small number of oligonucleotides. Therefore, we discarded from the data set the 281 genes for which 50% or more of the oligonucleotides targeting a gene showed a signal intensity of

<6 for at least one strain. This resulted in a final data set consisting of 88% of the 2,300 genes targeted in the microarray. Significant ($P < 0.01$) changes in expression exceeding $2\times$ (i.e., $|\log_2| > 1$) for at least one strain were considered differentially expressed (DE), resulting in 1,079 DE genes.

A similar transcriptomic response for all strains. Like CIRM-BIA1^T (6), the 6 strains downregulated most of the DE genes related to the general cell machinery, such as genes involved in energy production and protein synthesis, whereas both down- and upregulated genes were observed in some gene categories, like transport and metabolism of amino acids and carbohydrates (Fig. 2). The main features are briefly described below.

General slowdown of cell machinery and cold stress response. All strains slowed their metabolism, as indicated, for example, by the downregulation of *ftsX*, involved in cell division (fold changes ranging from -1.7 to -4.3) (Table 1), and of most of the genes involved in energetic metabolism (Table 1). Genes involved in the conversion of pyruvate into propionate (*sdhABC* and *pccB*) and into CO_2 and acetate (*aceE* and *lpd*) were also downregulated at 4°C (Table 1). Many bacteria exhibit a general

TABLE 1 Differentially expressed genes involved in general cell machinery slowdown

Name	Locus tag ^a	Description	Category ^b	P value		Fold change (log ₂) for CRM-BIA strain ^c									
				Time	Strain	Time × strain									
							118	122	123	1	472	482	9		
<i>csfA</i>	PEREUD_16500	Carbon starvation protein	A	<0.01	<0.01	<0.01	-1.0	-1.2	-3.4	-1.5	-2.0	-3.7	-2.9		
<i>fxsX</i>	PEREUD_09600	Cell division protein	CD	<0.01	<0.01	<0.01	-2.1	-1.7	-2.4	-4.7	-1.7	-3.8	-4.3		
<i>icd</i>	PEREUD_06870	Putative isocitrate/isopropylmalate dehydrogenase	CH	<0.01	<0.01	0.05	-1.0	-3.3	-2.0	-3.0	-3.4	-3.3	-3.0		
<i>pcdB</i>	PEREUD_07170	Propionyl-coenzyme A carboxylase beta chain	CH	<0.01	0.01	<0.01	-1.2	-1.6	-0.4	-1.8	-1.8	-1.5	-1.2		
<i>aceE</i>	PEREUD_09470	Pyruvate dehydrogenase E1 component	CH	<0.01	<0.01	0.14	-1.5	-1.9	-1.5	-1.9	-2.8	-2.1	-1.9		
<i>lpd</i>	PEREUD_10890	Dihydrolypyl dehydrogenase	CH	<0.01	0.28	0.44	-0.5	-0.9	-0.7	-1.5	-2.2	-0.8	-1.1		
<i>acn</i>	PEREUD_12590	Aconitase	CH	<0.01	<0.01	0.47	-0.7	-0.8	-1.0	-1.0	-1.5	-0.8	-1.0		
<i>cydA</i>	PEREUD_01720	Cytochrome <i>d</i> ubiquinol oxidase, subunit I	E	<0.01	<0.01	0.02	-0.8	-1.4	-1.6	-1.6	-1.5	-2.0	-3.4		
<i>cydB</i>	PEREUD_01730	Cytochrome <i>d</i> ubiquinol oxidase, subunit II	E	<0.01	<0.01	0.03	-1.0	-1.3	-1.3	-1.1	-0.7	-0.9	-2.2		
<i>nuoA</i>	PEREUD_05160	NADH-quinone oxidoreductase chain A	E	<0.01	<0.01	0.02	-1.4	-1.2	-0.5	-2.0	-1.3	-2.2	-2.0		
<i>nuoB</i>	PEREUD_05170	NADH-quinone oxidoreductase chain B	E	<0.01	<0.01	<0.01	-1.9	-1.8	-1.0	-2.3	-1.4	-3.3	-2.3		
<i>nuoC</i>	PEREUD_05180	NADH-quinone oxidoreductase chain C	E	<0.01	<0.01	<0.01	-1.9	-1.7	-1.3	-3.8	-2.3	-3.7	-3.4		
<i>nuoD</i>	PEREUD_05190	NADH-quinone oxidoreductase chain D	E	<0.01	<0.01	<0.01	-2.0	-1.9	-1.6	-3.8	-2.7	-4.9	-5.2		
<i>nuoE</i>	PEREUD_05200	NADH-quinone oxidoreductase chain E	E	<0.01	<0.01	<0.01	-2.0	-1.9	-1.9	-2.9	-2.5	-4.0	-3.3		
<i>nuoF</i>	PEREUD_05210	NADH-quinone oxidoreductase chain F	E	<0.01	<0.01	0.08	-2.2	-2.0	-1.9	-2.7	-2.4	-3.4	-2.9		
<i>nuoG</i>	PEREUD_05220	NADH-quinone oxidoreductase chain G	E	<0.01	<0.01	0.08	-2.0	-1.5	-1.9	-1.9	-2.2	-2.8	-3.1		
<i>nuoH</i>	PEREUD_05230	NADH-quinone oxidoreductase chain H	E	<0.01	<0.01	0.01	-1.8	-1.0	-1.6	-0.9	-1.6	-2.4	-1.7		
<i>nuoI</i>	PEREUD_05240	NADH-quinone oxidoreductase chain I	E	<0.01	<0.01	0.09	-2.5	-1.2	-1.6	-1.4	-2.3	-3.0	-2.9		
<i>nuoJ</i>	PEREUD_05250	NADH-quinone oxidoreductase chain J	E	<0.01	<0.01	0.02	-2.3	-1.1	-1.7	-1.5	-2.0	-3.3	-2.6		
<i>nuoK</i>	PEREUD_05260	NADH dehydrogenase I chain K	E	<0.01	<0.01	0.01	-2.5	-1.5	-2.1	-1.9	-2.5	-3.7	-2.9		
<i>nuoL</i>	PEREUD_05270	NADH dehydrogenase	E	<0.01	<0.01	0.01	-2.3	-1.1	-1.7	-1.3	-2.4	-3.2	-2.9		
<i>nuoM</i>	PEREUD_05280	NADH dehydrogenase I chain M	E	<0.01	<0.01	0.01	-2.3	-1.1	-1.7	-1.3	-2.4	-3.2	-2.9		
<i>nuoN</i>	PEREUD_05290	Succinate dehydrogenase I chain N	E	<0.01	<0.01	0.05	-1.3	-0.8	-2.1	-1.2	-2.2	-2.8	-2.2		
<i>sdhC1</i>	PEREUD_09240	Succinate dehydrogenase, subunit C	E	<0.01	<0.01	<0.01	-2.1	-1.2	0.5	-2.7	-2.9	-3.2	-3.4		
<i>sdhA</i>	PEREUD_09250	Succinate dehydrogenase, subunit A	E	<0.01	<0.01	<0.01	-2.1	-1.2	0.5	-2.7	-2.9	-3.2	-3.4		
<i>sdhB</i>	PEREUD_09260	Succinate dehydrogenase, subunit B	E	<0.01	<0.01	0.09	-1.2	-0.9	0.3	-0.9	-1.0	-0.7	-1.1		
<i>apbB</i>	PEREUD_10430	ATP synthase A chain	E	<0.01	<0.01	0.03	-2.0	-1.6	-1.5	-2.8	-2.6	-3.3	-2.5		
<i>apbE</i>	PEREUD_10440	ATP synthase B chain	E	<0.01	<0.01	0.22	-2.8	-2.7	-1.9	-3.1	-3.1	-2.8	-3.2		
<i>apbF</i>	PEREUD_10450	ATP synthase C chain	E	<0.01	<0.01	0.30	-2.9	-3.0	-2.1	-2.3	-2.7	-2.7	-2.6		
<i>apbH</i>	PEREUD_10460	ATP synthase delta chain	E	<0.01	0.25	0.06	-2.8	-2.8	-2.4	-3.4	-3.5	-3.0	-3.6		
<i>apbA</i>	PEREUD_10470	ATP synthase subunit alpha	E	<0.01	0.34	0.21	-3.0	-2.6	-2.5	-3.6	-3.6	-3.7	-3.5		
<i>apbG</i>	PEREUD_10480	ATP synthase gamma chain	E	<0.01	<0.01	0.20	-3.1	-2.6	-2.4	-3.7	-4.2	-3.9	-3.5		
<i>apbD</i>	PEREUD_10490	ATP synthase subunit beta	E	<0.01	0.05	0.38	-2.9	-2.3	-2.2	-3.0	-3.2	-3.1	-3.2		
<i>apbC</i>	PEREUD_10500	ATP synthase epsilon chain	E	<0.01	0.12	0.23	-3.8	-2.5	-2.4	-3.0	-3.6	-3.2	-3.8		
<i>sdhB3</i>	PEREUD_14300	Succinate dehydrogenase	E	<0.01	<0.01	0.02	-2.8	-2.6	-0.6	-2.4	-2.4	-2.7	-4.2		
<i>sdhA3</i>	PEREUD_14310	Succinate dehydrogenase flavoprotein subunit	E	<0.01	<0.01	<0.01	-2.5	-2.5	-0.3	-3.0	-2.2	-2.6	-4.3		
<i>sdhC2</i>	PEREUD_14320	Succinate dehydrogenase cytochrome B-558 subunit	E	<0.01	<0.01	<0.01	-2.4	-2.2	0.3	-2.3	-1.5	-2.3	-2.8		

^a Locus tag for CRM-BIA1^T.

^b A, adaptation to atypical conditions; CD, cell division; CH, transport and metabolism of carbohydrates; E, energy metabolism.

^c Values of |fold change (log₂)| > 1 are in boldface.

TABLE 2 Differentially expressed genes involved in cold stress response

Name	Locus tag ^a	Description	Category ^b	P value		Fold change (log ₂) for CIRM-BIA strain ^c							
				Time	Strain	Time × strain	118	122	123	1	472	482	9
<i>pspC</i>	PFREUD_06710	Possible stress response transcriptional regulator protein	A	<0.01	<0.01	<0.01	3.8	2.0	2.9	3.5	2.6	4.3	4.0
<i>pspC</i>	PFREUD_06710	Possible stress response transcriptional regulator protein	A	<0.01	<0.01	<0.01	3.8	2.0	2.9	3.5	2.6	4.3	4.0
<i>cspA</i>	PFREUD_09800	Cold shock-like protein	A	<0.01	<0.01	0.01	-0.3	0.1	1.6	2.1	1.3	1.7	1.9
<i>cspB</i>	PFREUD_18210	Cold shock protein	A	<0.01	<0.01	0.01	0.8	0.6	1.1	2.3	0.8	1.8	0.9
	PFREUD_04260	DeaD/DeaH box helicase	DNA	<0.01	<0.01	0.21	0.3	0.7	0.7	1.2	0.9	1.0	0.8
	PFREUD_13460	Superfamily II RNA helicase, DeaD/DeaH box helicase	DNA	<0.01	<0.01	0.04	1.3	1.2	1.5	2.0	0.9	1.9	1.8
<i>dnaK2</i>	PFREUD_04630	Chaperone protein	PM	<0.01	<0.01	<0.01	-0.5	-1.8	-2.6	-2.5	-2.5	-0.5	0.5
<i>grpE2</i>	PFREUD_04640	Co-chaperone protein	PM	<0.01	0.04	<0.01	0.9	-0.9	-1.5	-2.4	-1.5	0.0	0.9
<i>dnaJ2</i>	PFREUD_04650	Chaperone protein DnaJ2	PM	<0.01	<0.01	<0.01	-0.3	-0.9	-1.4	-1.1	-0.7	0.4	0.6
<i>groS1</i>	PFREUD_06460	10-kDa chaperonin 1	PM	<0.01	0.02	0.01	-2.4	-4.1	-3.9	-5.5	-5.4	-5.9	-5.2
<i>groL1</i>	PFREUD_06470	60-kDa chaperonin 1	PM	<0.01	0.24	0.22	-3.0	-3.9	-3.8	-4.0	-4.6	-4.9	-4.7
<i>groS2</i>	PFREUD_07810	10-kDa chaperonin 2	PM	<0.01	<0.01	0.15	-0.8	-0.6	0.3	-0.7	-1.1	-0.2	-0.8
<i>dnaJ3</i>	PFREUD_08760	Chaperone protein DnaJ3	PM	<0.01	<0.01	<0.01	-0.4	0.0	-0.6	-1.6	-1.3	-0.3	-0.8
<i>hsp20</i>	PFREUD_09500	Heat shock protein 20 2	PM	<0.01	0.03	0.03	-1.3	-0.6	-0.3	-0.1	-0.1	-0.6	1.2
<i>dnaJ1</i>	PFREUD_17820	Chaperone protein DnaJ1	PM	<0.01	<0.01	<0.01	-2.8	0.0	-2.2	-2.7	-1.6	-2.3	-2.2
<i>grpE1</i>	PFREUD_17830	Co-chaperone protein	PM	<0.01	<0.01	<0.01	-3.0	0.1	-2.8	-3.2	-2.0	-3.0	-2.3
<i>dnaK1</i>	PFREUD_17840	Chaperone protein	PM	<0.01	<0.01	<0.01	-2.9	0.2	-3.2	-2.0	-2.5	-4.5	-1.7
<i>clpB 2</i>	PFREUD_17920	Chaperone protein	PM	<0.01	<0.01	<0.01	-2.9	-0.4	-3.5	-3.3	-2.1	-1.9	-4.1
<i>groL2</i>	PFREUD_18470	60-kDa chaperonin 2	PM	<0.01	0.37	0.65	-2.9	-3.7	-3.2	-3.4	-3.3	-4.1	-3.6
<i>clpB 1</i>	PFREUD_19250	Chaperone protein	PM	<0.01	<0.01	<0.01	1.9	0.7	-1.3	0.8	0.2	2.7	1.2

^a Locus tag for CIRM-BIA1^T.
^b A, adaptation to atypical conditions; DNA, DNA metabolism; PM, protein modification and folding.
^c Values of [fold change (log₂)] >1 are in boldface.

TABLE 3 Genes encoding esterases and branched-chain amino acid-converting enzymes

Type of enzyme and name	Locus tag ^a	Description ^b	Category ^c	P value			Fold change (log ₂) for each CIRM-BIA strain ^d								
				Time	Strain	Time × strain	118	122	123	1	472	482	9		
Esterases															
<i>pfl861</i>	PFREUD_03560	Putative carboxylic ester hydrolase	L	0.18	<0.01	0.06	−0.2	−0.6	−0.4	0.2	0.4	0.2	−0.6		
<i>pfl774</i>	PFREUD_04240	Putative carboxylic ester hydrolase	L	0.60	<0.01	0.11	0.4	−0.7	−0.4	0.3	0.2	0.2	−0.3	0.6	
<i>pfl729</i>	PFREUD_04340	Carboxylic ester hydrolase	L	0.32	0.01	0.11	0.3	−0.6	−0.6	0.6	0	0.1	0.4	0.4	
<i>pfl962</i>	PFREUD_04810	Carboxylic ester hydrolase	L	<0.01	0.05	0.61	0.5	0.4	0.5	0.7	0.2	0.2	0.5	0.2	
<i>pfl509</i>	PFREUD_10540	Putative carboxylic ester hydrolase	L	0.50	<0.01	0.03	0.0	0.5	0.2	0.3	−0.7	0.9	−0.5	−0.5	
<i>pfl758-2887</i>	PFREUD_10790- PFREUD_10800	Putative carboxylic ester hydrolases ^e	L	0.57	0.02	0.34	−0.3	−0.2	−0.3	— ^c	0.2	0.2	0.5	— ^c	
<i>pfl637</i>	PFREUD_12910	Putative carboxylic ester hydrolase	L	<0.01	<0.01	0.07	0.0	−0.4	0.3	0.0	−0.8	−0.3	−0.4	−0.4	
<i>pfl739</i>	PFREUD_13000	Putative carboxylic ester hydrolase	L	<0.01	<0.01	<0.01	0.8	0.7	0.6	1.2	0.6	0.6	1.6	0.6	
<i>pfl69</i>	PFREUD_14330	Carboxylic ester hydrolase	L	0.13	0.19	0.13	−0.1	−0.2	−0.1	0.3	0.1	0.5	0.1	0.1	
<i>pfl655</i>	PFREUD_18110	Carboxylic ester hydrolase	L	0.59	<0.01	0.55	0.3	0.7	−0.4	−0.1	0	0	−0.3	−0.3	
<i>pfl667</i>	PFREUD_23150	Carboxylic ester hydrolase	L	<0.01	<0.01	<0.01	0.1	−0.1	0.2	0.9	0.3	0.5	0.5	−0.2	
<i>pfl2042</i>	PFREUD_23770	Putative carboxylic ester hydrolase	L	<0.01	<0.01	0.04	−0.3	−0.6	−0.6	−0.2	0.1	0.1	−0.6	−0.4	
Branched-chain amino acid transport and conversion															
<i>livG</i>	PFREUD_10850	ABC protein of branched-chain amino acid ABC transporter	AA	<0.01	<0.01	0.02	−1.4	−0.8	−2.3	−3.6	−2.4	−3	−2.1	−2.1	
<i>braE</i>	PFREUD_10860	IM protein of branched-chain amino acid ABC transporter	AA	<0.01	<0.01	<0.01	−0.5	−0.3	−0.8	−1.5	−1.1	−1.5	−0.6	−0.6	
<i>braD</i>	PFREUD_10870	IM protein of branched-chain amino acid ABC transporter	AA	<0.01	<0.01	<0.01	−1.0	−0.4	−1.3	−1.9	−1	−2.4	−0.9	−0.9	
<i>braC</i>	PFREUD_10880	BP of branched-chain amino acid ABC transporter	AA	<0.01	<0.01	0.01	−1.0	−0.5	−1.2	−2.9	−1.6	−2.2	−0.6	−0.6	
<i>ydaO</i>	PFREUD_12690	IM protein of branched-chain amino acid ABC transporter	AA	<0.01	<0.01	0.06	−2.1	−2	−1.6	−2.4	−1.9	−2.4	−2.2	−2.2	
<i>ilvE</i>	PFREUD_13350	Branched-chain amino acid aminotransferase	AA	0.45	0.01	0.10	−0.2	0.2	−0.4	0.3	−1.5	0.4	0.4	0.4	
<i>bkdA2</i>	PFREUD_02200	2-Oxoisovalerate dehydrogenase subunit beta	AA	<0.01	<0.01	0.03	−2.1	−3.7	−2.0	−3.3	−3.3	−3.5	−3.9	−3.9	
<i>bkdB</i>	PFREUD_02210	Dihydrolipoylysine residue (2-methylpropanoyl) transferase	AA	<0.01	<0.01	0.03	−0.8	−1.7	−0.7	−1.8	−1.4	−0.7	−1.5	−1.5	

^a Locus tag for CIRIM-BIAI^T.^b IM, integral membrane; BP, binding protein.^c L, lipid metabolism; AA, transport and metabolism of amino acids.^d Values of fold change (log₂) > 1 are in boldface.^e This gene presents a frameshift in strains CIRIM-BIAI^T and CIRIM-BIA9.

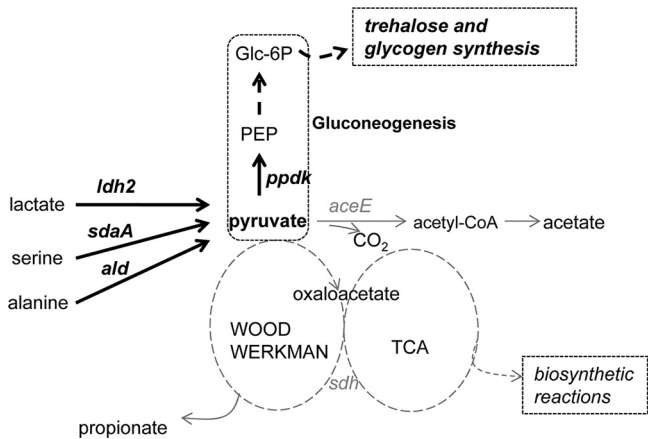


FIG 3 Main routes of pyruvate formation and conversion in *P. freudenreichii* during storage at 4°C and relevant for this study. Genes upregulated at 4°C are shown in black, and downregulated genes in gray. Thick black arrows emphasize the metabolic pathways that are favored at 4°C, and thin gray arrows the pathways that are downregulated at 4°C. *ace*, pyruvate dehydrogenase, E1 component; *ald*, alanine dehydrogenase; *ldh*, L-lactate dehydrogenase; *ppdk*, pyruvate phosphate dikinase; *sdaA*, L-serine dehydratase; *sdh*, succinate dehydrogenase; CoA, coenzyme A. Values of fold changes are shown in Table 1, Table 4, and Fig. 5.

slowdown in the cold; for example, *Lactococcus lactis* in model cheeses when placed at 12°C (5). The 6 strains exhibited cold stress responses similar to those of CIRM-BIA1^T (6) and other bacteria (2, 15). For example, the genes *cspA* and *cspB*, encoding cold shock proteins, were upregulated, as well as DEAD box RNA helicases, which facilitate translation and, thus, protein synthesis in the cold (Table 2). In contrast, several chaperone- and heat shock protein-

coding genes (*groSL* and *dnaKJ* operons and *hsp20*, *clpB2*, and *grpE*) were downregulated at 4°C for most strains (Table 2).

Production of aroma compounds in the cold. *P. freudenreichii* contributes to the development of Swiss cheese flavor via different pathways involving esterases and branched-chain amino acid-converting enzymes (16). The 12 esterase-encoding genes identified in the *P. freudenreichii* genome (8), in particular *pf279*, encoding a lipolytic secreted esterase probably involved in lipolysis (9), kept the same level of expression at 4°C in the 6 strains tested, as previously observed for CIRM-BIA1^T (Table 3). These results are in agreement with the observation that *P. freudenreichii* still contributes to the formation of free fatty acids in cheese at low temperatures (16). Most genes encoding branched-chain amino acid transporters and converting enzymes were downregulated (for example, fold changes ranging from −2.0 to −3.9 for *bkdA2*) (Table 3), whereas methylbutanoate was still produced at 4°C (Fig. 1B). It suggests that this pathway is posttranscriptionally regulated and/or that branched-chain amino acid-converting enzymes were accumulated in cells and remained active at 4°C.

Rerouting of carbon metabolism toward glycogen synthesis. The phosphoenolpyruvate-pyruvate-oxaloacetate node interconnects the major pathways of carbon metabolism in bacteria (13). The main changes in the expression of pyruvate-related genes in *P. freudenreichii* in the cold are shown in Fig. 3. Three genes involved in generating pyruvate from alanine, serine, and lactate were upregulated, as previously observed in CIRM-BIA1^T (6), as well as genes involved in gluconeogenesis (*ppdk*, *eno1*, *eno2*, *fba2*, and *pgi*) (Table 4). PpdK is a pyrophosphate-dependent enzyme, and accordingly, an inorganic pyrophosphatase-coding gene was found to be overexpressed in the cold in all strains (*ppa*) (Table 4). Genes coding for enzymes of glycogen synthesis by the classical *pgmA*-*glgC*-*glgA* pathway were overexpressed (Fig. 4). Moreover,

TABLE 4 Differentially expressed genes involved in pyruvate generation and rerouting toward trehalose and glycogen synthesis

Function and name	Locus tag ^a	Description	Category ^b	P value			Fold change (log ₂) for each CIRM-BIA strain ^c						
				Time	Strain	Time × Strain	118	122	123	1	472	482	9
Generation of energy													
<i>ppa</i>	PFREUD_23500	Inorganic pyrophosphatase	Ph	<0.01	<0.01	<0.01	2.5	1.8	1.7	3.3	2.7	2.8	2.5
Generation of pyruvate													
<i>ald</i>	PFREUD_00370	Alanine dehydrogenase	AA	<0.01	<0.01	<0.01	3.7	4.5	1.1	7.5	3.2	2.0	4.3
<i>sdaA</i>	PFREUD_18570	L-Serine dehydratase	AA	<0.01	<0.01	<0.01	1.6	1.3	0.5	2.0	1.0	1.9	0.9
<i>ldh2</i>	PFREUD_12840	L-Lactate dehydrogenase	CH	<0.01	0.02	0.01	1.5	2.0	1.3	1.3	1.7	1.8	0.4
Gluconeogenesis													
<i>ppdk</i>	PFREUD_03230	Pyruvate phosphate dikinase	CH	<0.01	<0.01	<0.01	1.3	1.2	−0.6	1.9	0.9	0.3	0.6
<i>eno1</i>	PFREUD_17320	Enolase 1	CH	<0.01	<0.01	0.01	1.1	1	0.6	2.6	1.9	1.7	1.1
<i>eno2</i>	PFREUD_17250	Enolase 2	CH	<0.01	<0.01	0.02	1.2	1.2	0.7	0.6	1.3	1.1	0.7
<i>fba1</i>	PFREUD_19150	Fructose-bisphosphate aldolase class II	CH	<0.01	<0.01	0.33	−0.5	−1.2	−0.3	−1.0	−0.7	−0.6	−1.0
<i>fba2</i>	PFREUD_23890	Fructose-bisphosphate aldolase class I	CH	<0.01	<0.01	<0.01	2.5	2.4	0.5	3.9	2.3	1.2	2.2
<i>pgi</i>	PFREUD_04290	Glucose-6-phosphate isomerase	CH	<0.01	<0.01	<0.01	1.0	0.4	0.5	1.6	0.8	1.2	1.5

^a Locus tag in CIRM-BIA1^T.
^b Ph, metabolism of phosphate; AA, transport and metabolism of amino acids; CH, transport and metabolism of carbohydrates.
^c Values of |fold change (log₂)| > 1 are in boldface.

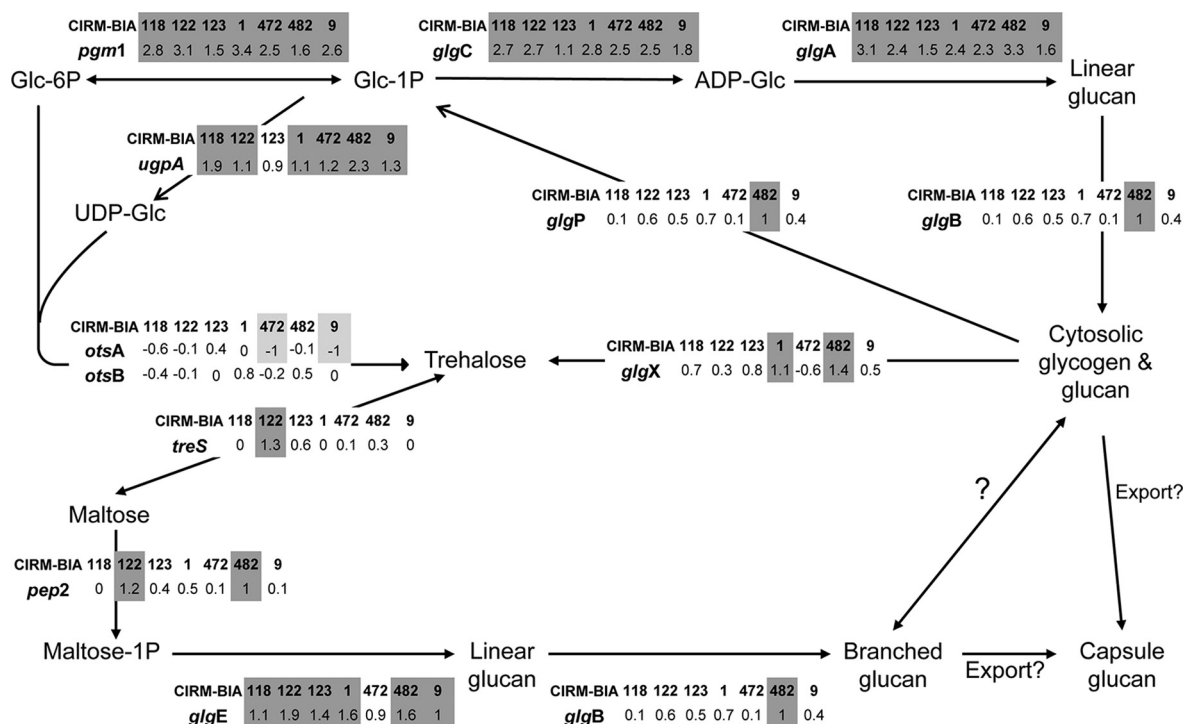


FIG 4 Changes in expression of genes involved in trehalose and glycogen synthesis in *P. freudenreichii* (pathways adapted from Chandra et al. [3]). Each box shows the fold change, expressed as log₂, for each gene in all seven strains (CIRM-BIA118, -122, -123, -1, -472, -482, and -9) after 80 h at 4°C in comparison with gene expression at the reference time (20 h). Values of |fold change (log₂)| > 1 and < -1 are shown in dark and light gray, respectively.

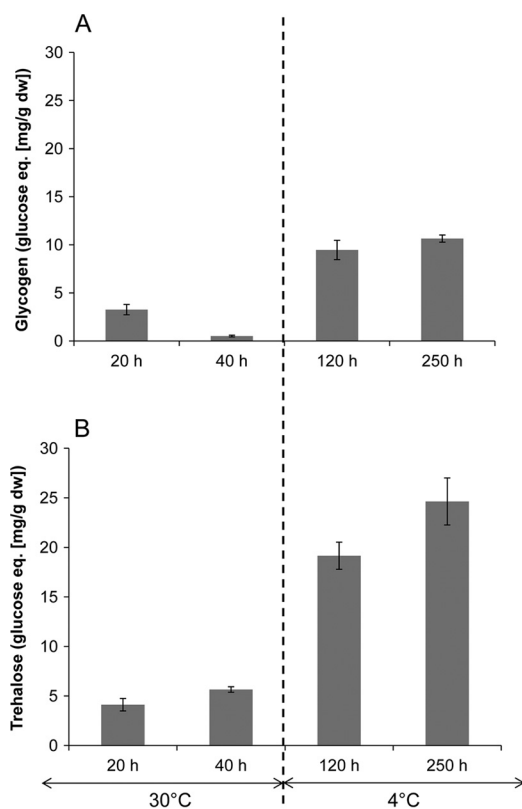


FIG 5 Accumulation of intracellular glycogen and trehalose in *P. freudenreichii* CIRM-BIA1^T during growth at 30°C (up to 40 h of incubation) and further incubation for 250 h at 4°C. Values are means of the results of triplicate independent experiments; error bars show standard deviations. eq, equivalent.

we showed that *glgE*, encoding a maltosyltransferase, present in the newly described *treS-pep2-glgE* pathway of glycogen synthesis from trehalose in mycobacteria (3), was also upregulated in all of the strains (fold changes ranging from 0.9 to 1.4) (Fig. 4). To confirm that glycogen was effectively synthesized by *P. freudenreichii*, it was quantified in cells over the incubation time (incubation at 4°C extended for 250 h), along with trehalose, since the syntheses of these two compounds are interconnected (3). Both compounds were analyzed in CIRM-BIA1^T cells by enzymatic methods as previously described (12). Our results showed that the concentrations of glycogen and trehalose increased by factors of 3 and 18, respectively, between the end of growth at 30°C (40 h) and 120 h of incubation at 4°C (Fig. 5). The present study provides the first quantification of glycogen accumulation in propionibacteria, confirms the results of an *in vivo* ¹³C nuclear magnetic resonance (NMR) study showing the ability of the same strain to synthesize glycogen (11), and shows that low temperature and not only nutrient starvation can induce the synthesis of glycogen in bacteria. The synthesis of trehalose by propionibacteria was early reported (14), with O₂, NaCl, and pH stresses known to induce its synthesis in propionibacteria (1).

Conclusions. This study shows that adaptation strategies in the cold described for the type strain are general within *P. freudenreichii* species and gives clues on the molecular basis of the long-term survival and activity of this bacterium during prolonged incubation at low temperatures.

ACKNOWLEDGMENTS

We thank Pascal Pachot, Stat-Plan, for his support concerning statistical analysis and Victoria Chuat (CIRM-BIA, INRA, Rennes, France) for strain preparations.

INRA, Valio Ltd. (Helsinki, Finland), and Tekes (the Finnish Funding Agency for Technology and Innovation) supported this study.

REFERENCES

- Cardoso FS, Gaspar P, Hugenholtz J, Ramos A, Santos H. 2004. Enhancement of trehalose production in dairy propionibacteria through manipulation of environmental conditions. *Int. J. Food Microbiol.* **91**: 195–204.
- Chan YC, Wiedmann M. 2009. Physiology and genetics of *Listeria monocytogenes* survival and growth at cold temperatures. *Crit. Rev. Food Sci. Nutr.* **49**:237–253.
- Chandra G, Chater KF, Bornemann S. 2011. Unexpected and widespread connections between bacterial glycogen and trehalose metabolism. *Microbiol.* **157**:1565–1572.
- Cousin F, Mater DDG, Foligné B, Jan G. 2 August 2010. Dairy propionibacteria as human probiotics: a review of recent evidence. *Dairy Sci. Technol.* <http://dx.doi.org/10.1051/dst/2010032>.
- Cretenet M, et al. 2011. Dynamic analysis of the *Lactococcus lactis* transcriptome in cheeses made from milk concentrated by ultrafiltration reveals multiple strategies of adaptation to stresses. *Appl. Environ. Microbiol.* **77**:247–257.
- Dalmasso M, et al. 2012. A temporal -omic study of *Propionibacterium freudenreichii* CIRM-BIA1T adaptation strategies in conditions mimicking cheese ripening in the cold. *PLoS One* **7**:e29083. doi:10.1371/journal.pone.0029083.
- Dalmasso M, et al. 2011. Multilocus sequence typing of *Propionibacterium freudenreichii*. *Int. J. Food Microbiol.* **145**:113–120.
- Dherbécourt J, Falentin H, Canaan S, Thierry A. 2008. A genomic search approach to identify esterases in *Propionibacterium freudenreichii* involved in the formation of flavour in Emmental cheese. *Microb. Cell Fact.* **7**:16. doi:10.1186/1475-2859-7-16.
- Dherbécourt J, et al. 2010. Identification of a secreted lipolytic esterase in *Propionibacterium freudenreichii*, a ripening process bacterium involved in Emmental cheese lipolysis. *Appl. Environ. Microbiol.* **76**:1181–1188.
- Falentin H, et al. 2010. Specific metabolic activity of ripening bacteria quantified by real-time reverse transcription PCR throughout Emmental cheese manufacture. *Int. J. Food Microbiol.* **144**:10–19.
- Meurice G. 2004. Biochimie, biologie cellulaire et moléculaire. Ph.D. thesis. Ecole Nationale Supérieure Agronomique de Rennes, Rennes, France.
- Parrou JL, Francois J. 1997. A simplified procedure for a rapid and reliable assay of both glycogen and trehalose in whole yeast cells. *Anal. Biochem.* **248**:186–188.
- Sauer U, Eikmanns BJ. 2005. The PEP-pyruvate-oxaloacetate node as the switch point for carbon flux distribution in bacteria. *FEMS Microbiol. Rev.* **29**:765–794.
- Stjernholm R. 1958. Formation of trehalose during dissimilation of glucose by *Propionibacterium*. *Acta Chem. Scand.* **12**:646–649.
- Thieringer HA, Jones PG, Inouye M. 1998. Cold shock and adaptation. *Bioessays* **20**:49–57.
- Thierry A, et al. 2011. New insights into physiology and metabolism of *Propionibacterium freudenreichii*. *Int. J. Food Microbiol.* **149**:18–27.